

Firn densification model

Douglas Brinkerhoff

Evan Cummings

Tyler Davis

Jesse Johnson

January 14, 2013



1 Introduction

The top layer of snow on a glacier or ice sheet increases in density as depth increases; newly accumulated snow builds up and compresses the layers below. *Herron and Langway* [1980] developed a firn densification model based on Arrhenius-type equations with variable rate constants, and found that the densification rate decreased suddenly around 550 kg m^{-3} . *Zwally and Li* [2002] expanded upon this model and found an alternate temperature-dependent value for the rate constant. *Arthern et al.* [2010] developed yet another set of equations based from their in situ measurements of Antarctic snow compaction. *Ligtenberg et al.* [2011] modified the *Arthern et al.* [2010] parametrization to better fit areas with a higher average annual temperature.

We have re-created a number of these models and integrated them with an enthalpy-formulation proposed by *Aschwanden et al.* [2012] which accounts for melting of firn layers in percolation zones. The model simulates ice lenses formed from within the firn column, and work is currently being done to allow the movement of water through the column. The model has been created with the finite-element software package FEniCS; an explanation of its usage and flexibility will be made clear.

2 Temperature Solution

We begin with the standard heat-transport equation as explained by *Patterson* [2001]

$$\rho c_i \frac{\partial T}{\partial t} = k_i \frac{\partial^2 T}{\partial z^2} + \left(\frac{dk_i}{dt} - \rho c_i w \right) \frac{\partial T}{\partial z}$$

with heat sources from the deformation of ice omitted, ρ density, c_i heat capacity, k_i thermal conductivity, w vertical velocity, and T temperature of firn. To solve the total derivative dk_i/dt we must apply the chain rule

$$\frac{dk_i}{dz} = \frac{\partial k_i}{\partial \rho} \frac{\partial \rho}{\partial z} + \frac{\partial k_i}{\partial T} \frac{\partial T}{\partial z}.$$

The thermal conductivity of ice is defined by *Arthern et al.*, 1998 as

$$k_i = 2.1 \left(\frac{\rho}{\rho_i} \right)^2,$$

from which we find

$$\frac{\partial k_i}{\partial \rho} = 4.2 \frac{\rho}{\rho_i^2}$$

and

$$\frac{\partial k_i}{\partial T} = \frac{4.2}{\rho_i^2} \left(\frac{\partial \rho}{\partial T} \right).$$

Patterson [2001] defined the heat capacity c_i of firn with the equation

$$c_i = 152.5 + 7.122T,$$

where we make $T = T_{avg}$ to simplify calculations. Contained within the same literature is an expression ρ in terms of T which leads to the equation:

$$\frac{\partial \rho}{\partial T} = (5.6 \times 10^{-2}) \exp((-5.7 \times 10^{-3})T).$$

The vertical velocity of ice w can be described with the differential equation

$$\frac{\partial w}{\partial z} = \frac{1}{\rho} \frac{d\rho}{dt}.$$

3 Density Solution

The densification process is defined with the material derivative

$$\frac{d\rho}{dt} = \frac{\partial \rho}{\partial t} + w \frac{\partial \rho}{\partial z}.$$

Arthern et al. [2010] described this derivative differently for density values above and below a critical value, ρ_m :

$$\frac{d\rho}{dt} = \begin{cases} c_0(\rho_i - \rho), & \rho \leq \rho_m \\ c_1(\rho_i - \rho), & \rho > \rho_m \end{cases}.$$

Zwally and Li [2002] defined a single multiplying constant c with an Arrhenius-type relation

$$c_0 = c_1 = \dot{b}\beta(T) \left(\frac{\rho_i}{\rho_w} \right) K_{0G}(T) \exp\left(-\frac{E(T)}{RT}\right),$$

with $K_{0G}(T) \exp(-E(T)/(RT)) = 8.36T^{-2.061}$ as described in *Reeh* [2008], average annual accumulation rate \dot{b} in units of $\text{kg m}^{-2} \text{ s}^{-1}$, and $\beta(T)$ a unit-less smoothing function to match a desired density rate. *Arthern et al* [2010] developed a semi-empirical formula by coupling the rate equations for Nabarro-Herring creep and normal grain-growth:

$$\begin{cases} c_0 = M_0 \dot{b} g \frac{k_{c0}}{k_g} \exp\left(-\frac{E_c}{RT} + \frac{E_g}{RT_{avg}}\right) \\ c_1 = M_1 \dot{b} g \frac{k_{c1}}{k_g} \exp\left(-\frac{E_c}{RT} + \frac{E_g}{RT_{avg}}\right) \end{cases},$$

with the creep coefficients defined as

$$\begin{cases} k_{c0} = 9.2 \times 10^{-9} \text{ m}^3 \text{ s kg}^{-1} \\ k_{c1} = 3.7 \times 10^{-9} \text{ m}^3 \text{ s kg}^{-1} \end{cases}$$

and M defined in *Ligtenberg et al.* [2011] to better fit with observed densification rates in higher-temperature environments:

$$\begin{cases} M_0 = 2.366 - 0.293 \ln(\dot{b} * 1 \times 10^3) \\ M_1 = 1.435 - 0.151 \ln(\dot{b} * 1 \times 10^3) \end{cases}.$$

4 Enthalpy Solution

As stated in *Aschwanden et al.* [2012], we take 'enthalpy' to be synonymous with 'internal energy' due to the exclusion of work done with changing volume. The equation used here is the shallow-enthalpy:

$$\rho \frac{\partial H}{\partial t} = \frac{\partial}{\partial z} \left(\left\{ \begin{array}{cc} K_i, & \text{Temperate} \\ K_0, & \text{Cold} \end{array} \right\} \frac{\partial H}{\partial z} \right) + w \rho \frac{\partial H}{\partial z}.$$

Strain heating has been neglected and the advective term $w \rho \partial H / \partial z$ has been added. The coefficient for temperate ice is

$$K_i = \frac{k_i}{c_i},$$

and the coefficient for cold ice is

$$K_0 = \frac{1}{10} K_i.$$

Temperate firm is defined as firm with $H > H_s$, cold firm with $H \leq H_s$, where

$$H_s = \int_{T_0}^{T_m} c_i(T) dT,$$

with $T_m = 273.15$ K and $T_0 = 0.0$ K. The enthalpy can be found with a constant heat capacity of $2009 \text{ J kg}^{-1} \text{ K}^{-1}$ by the linear equation

$$H = \begin{cases} c_i(T - T_0), & \text{where } T \leq T_m \\ c_i(T_w - T_0) + \omega L_f, & \text{where } T > T_m \end{cases}$$

where L_f is the latent heat of fusion and ω represents the water content percentage of firm given by

$$\omega L_f = H - c_i(T_w - T_0).$$

Temperature may be derived from enthalpy easily:

$$T = \frac{H}{c_i}.$$

The density of the firm column changes with the percentage of water content:

$$\rho^n = \begin{cases} \rho^{n-1} + \Delta\omega(\rho_w - \rho_i) \text{ kg m}^{-3}, & \Delta\omega \leq 0 \\ \rho^{n-1} + \Delta\omega \rho_w \text{ kg m}^{-3}, & \Delta\omega > 0 \end{cases},$$

where $\Delta\omega = \omega^n - \omega^{n-1}$ is the change in water content and superscripts refer to the time index. This has the effect of adding water to the firm column and refreezing the portion of firm with decreasing water content. The surface-density at time index $n + 1$ can be described as:

$$\rho_s^{n+1} = \rho_b^{n+1} d_p + \rho_s^n (1 - d_p),$$

where

$$\begin{aligned} \rho_b^{n+1} &= \rho_b^{n-1} + \Delta\omega_s \rho_b^n, \\ \Delta\omega_s &= \omega_s^n - \omega_s^{n-1}, \\ d_p &= \frac{d_n}{l_s}, \\ d_n &= w_s \Delta t, \text{ and} \\ l_s &\text{ is the length of the surface node.} \end{aligned}$$

If $T_s \geq T_w$, the density of surface snow while taking into account re-freezing is simulated making

$$\rho_b^n = \begin{cases} \rho_w - \rho_i \text{ kg m}^{-3}, & \Delta\omega_s < 0 \\ \rho_w \text{ kg m}^{-3}, & \Delta\omega_s > 0 \end{cases},$$

but when $T_s < T_w$, ρ_b^n is simply made to be ρ_s .

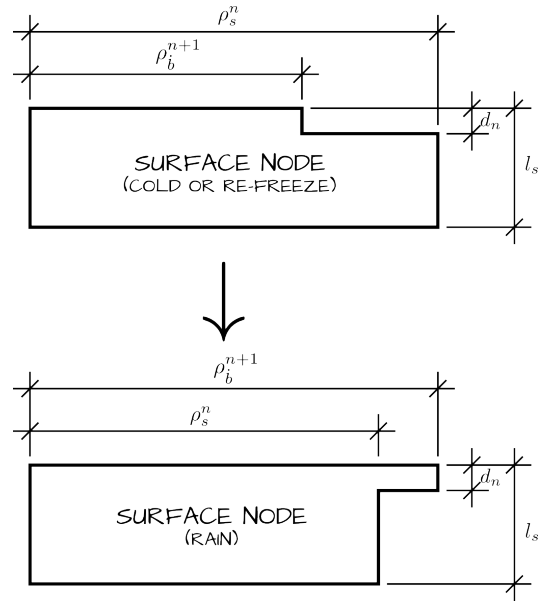


Figure 1: Evolution of surface node density

5 Finite Element Method

This section will focus on the enthalpy solution. Solving these equations with FEniCS is done with Galerkin's method and requires finding the weak formulation:

$$\begin{aligned} 0 &= \int_{\Omega} \left\{ \begin{array}{c} K_i \\ K_0 \end{array} \right\} \nabla^2 H \psi \, d\Omega + \int_{\Omega} w \rho \nabla H \psi \, d\Omega \\ &\quad - \int_{\Omega} \rho \frac{\partial H}{\partial t} \psi \, d\Omega. \end{aligned}$$

Here we have integrated the enthalpy equation over the entire domain, Ω , and multiplied by a test function ψ . Af-

ter integrating the diffusive term by parts this becomes

$$f_H = - \int_{\Omega} \left\{ \frac{K_i}{K_0} \right\} \nabla H \nabla \psi \, d\Omega + \int_{\Omega} w \rho \nabla H \psi \, d\Omega - \int_{\Omega} \rho \frac{\partial H}{\partial t} \psi \, d\Omega.$$

We can discretize the enthalpy time-differential with the second-order accurate formula

$$\frac{\partial H}{\partial t} = \frac{H - H^{k-1}}{\Delta t} = \theta H^k + (1 - \theta) H^{k-1}$$

with superscripts referring to time index. Using a θ -scheme as given by *Logg et al.* [2011], $H_{mid} = \theta H^k + (1 - \theta) H^{k-1}$, where $\theta \in [0, 1]$ is a weighting factor chosen from:

$$\theta = \begin{cases} 1, & \text{Backwards-Euler} \\ 0.667, & \text{Galerkin} \\ 0.878, & \text{Liniger} \\ 0.5, & \text{Crank-Nicolson} \\ 0, & \text{Forward-Euler} \end{cases}$$

The entire enthalpy residual can be represented in FEniCS as:

```
theta = 0.5
H_mid = theta*H + (1 - theta)*H_1
f_H = rho*(H - H_1)/dt*psi*dx +
      k/c*Kcoef*
      inner(grad(H_mid), grad(psi))*dx +
      rho*w*grad(H_mid)*psi*dx
```

The variable $Kcoef$ is a coefficient vector which will be updated dynamically depending on the temperature of firm (either 1.0 or 0.1 corresponding to K_i and K_0).

The weak form for density is found similarly, with a upwinding necessary to eliminate artifacts due to the sudden increase in density where ice lenses formed. The method used here is the Streamline Upwind Petrov-Galerkin (SUPG) method:

$$\hat{\phi} = \phi + \frac{h}{2||w||} w \cdot \nabla \phi,$$

where h is the cellsize. The density residual after integration by parts becomes:

$$f_\rho = \int_{\Omega} \frac{\partial \rho}{\partial t} \phi \, d\Omega + \int_{\Omega} w \nabla \rho \hat{\phi} \, d\Omega - \int_{\Omega} \frac{d\rho}{dt} \hat{\phi} \, d\Omega.$$

With the partial-time differential of density defined identically to the enthalpy equation, this can be represented in FEniCS including the *Arthern et al.* [2010] densification equation as:

```
vnorm = sqrt(dot(w, w) + 1e-10)
cellh = CellSize(mesh)
phi_hat = phi + cellh/(2*vnorm)*dot(w, grad(phi))
c = b*g*rhoCoef/kg *
    exp(-Ec/(R*T) + Eg/(R*Tavg))
drhodt = c*(rho_i - rho)
theta = 1.0
rho_mid = theta*rho + (1 - theta)*rho_1
f_rho = (rho - rho_1)/dt*phi*dx -
        (drhodt - w*grad(rho_mid))*phi_hat*dx
```

The variable $\rho Coef$ is another dynamically-updated-coefficient vector and is either k_{c0} or k_{c1} depending upon the density at the node. We have chosen $\theta = 1$ corresponding to the Backwards-Euler method due to the jump condition at ρ_m .

In order to find the vertical velocity the differential equation must be solved. The weak formulation is:

$$f_w = \int_{\Omega} \rho \nabla w \eta \, d\Omega + \frac{d\rho}{dt} \eta \, d\Omega,$$

and is created with FEniCS by:

```
theta = 1.0
w_mid = theta*w + (1 - theta)*w_1
f_w = rho*grad(w_mid)*eta*dx + drhodt*eta*dx
```

We chose $\theta = 1$ again due to the jump discontinuity at ρ_m .

We can define the function space for the entire non-linear problem as

$$U = \Omega \times \Omega \times \Omega,$$

with corresponding trial and test functions respectively defined as

$$d_h, j \subset U.$$

The test functions for each function can now be described as

$$\psi, \phi, \eta \subset j.$$

In FEniCS these spaces can be defined by this:

```
mesh = IntervalMesh(n, zb, zs)
V = FunctionSpace(mesh, 'Lagrange', 1)
MV = MixedFunctionSpace([V, V, V])
h = Function(MV)
H, rho, w = split(h)
dh = TrialFunction(MV)
dH, drho, dw = split(dh)
j = TestFunction(MV)
psi, phi, eta = split(j)
```

The variable zb is the z-position of the base of the firm column which does not change and n is the number of nodes; the $mesh$ variable defines the spacial dimensions of the system to be solved and is here created in one dimension. The $mesh$ may also be created in three dimensions if desired, or made to fit a custom grid. The variables dH and $drho$ are the trial functions for the enthalpy and density functions and are not utilized in this code, but are included for reference later on.

We define the complete non-linear residual as

$$f = f_H + f_\rho + f_w.$$

Solving this system can be accomplished with *Newton's Method* which requires derivation of the Jacobian:

$$J = \frac{\partial f}{\partial d_h}.$$

In FEniCS this is done with:

```
f = f_H + f_rho + f_w
J = derivative(f, h, dh)
```

6 Age Solution

The age of firm is described with the equation

$$\frac{\partial a}{\partial t} = 1 - w \nabla a.$$

Because this equation is purely advective, upwinding is needed; the method chosen here is *Taylor-Galerkin* and is described in *Codina* [1997]. The Taylor series expansion of w is

$$a^{k+1} = a^k + \frac{\partial a^k}{\partial t} \Delta t + \frac{1}{2} \frac{\partial^2 a^{k+\theta}}{\partial t^2} \Delta t^2 + O(\Delta t^3).$$

Replacing the time partials with the previous equation and eliminating the Δt^3 term, we have

$$a^{k+1} = a^k + [1 - w \nabla a^k] \Delta t - \frac{1}{2} \frac{\partial}{\partial t} [1 - w \nabla a^{k+\theta}] \Delta t^2.$$

Rearranging and simplifying,

$$\frac{a^{k+1} - a^k}{\Delta t} = 1 - w \nabla a^k - \frac{w \Delta t}{2} \left(\nabla \frac{\partial a^{k+\theta}}{\partial t} \right).$$

The time differential in the last term can again be replaced,

$$\frac{a^{k+1} - a^k}{\Delta t} = 1 - w \nabla a^k - \frac{w \Delta t}{2} (\nabla [1 - w \nabla a^{k+\theta}]),$$

reduced to

$$\frac{a^{k+1} - a^k}{\Delta t} = 1 - w \nabla a^k + \frac{w \Delta t}{2} (\nabla [w \nabla a^{k+\theta}]),$$

and finally evaluated using the product rule as

$$\begin{aligned} \frac{a^{k+1} - a^k}{\Delta t} = & 1 - w \nabla a^k \\ & + \frac{w \Delta t}{2} (w \nabla^2 a^{k+\theta} + \nabla w \nabla a^{k+\theta}). \end{aligned}$$

After moving all the terms to one side, multiplying by the test function ξ , and integrating over Ω we have

$$\begin{aligned} 0 = & \int_{\Omega} \frac{a^{k+1} - a^k}{\Delta t} \xi \, d\Omega - \int_{\Omega} 1 \xi \, d\Omega + \int_{\Omega} w \nabla a^k \xi \, d\Omega \\ & - \int_{\Omega} \frac{w^2 \Delta t}{2} \nabla^2 a^{k+\theta} \xi \, d\Omega - \int_{\Omega} \frac{w \Delta t}{2} \nabla w \nabla a^{k+\theta} \xi \, d\Omega. \end{aligned}$$

Integrating the second to last term by parts and disregarding the boundary term results in

$$\begin{aligned} 0 = & \int_{\Omega} \frac{a^{k+1} - a^k}{\Delta t} \xi \, d\Omega - \int_{\Omega} 1 \xi \, d\Omega + \int_{\Omega} w \nabla a^k \xi \, d\Omega \\ & + \int_{\Omega} \frac{w^2 \Delta t}{2} \nabla a^{k+\theta} \cdot \nabla \xi \, d\Omega - \int_{\Omega} \frac{w \Delta t}{2} \nabla w \nabla a^{k+\theta} \xi \, d\Omega. \end{aligned}$$

This final residual may be created in fenics as:

```
a = Function(V)
da = TrialFunction(V)
xi = TestFunction(V)
a_1 = Function(V)

theta = 0.5
a_mid = theta*a + (1-theta)*a_1
f_a = (a - a_1)/dt*xi*dx
      - 1.*xi*dx
      + w*grad(a_mid)*xi*dx
      + w**2*dt/2*grad(a_mid)*grad(xi)*dx
      - w*grad(w)*dt/2*grad(a_mid)*xi*dx
```

7 Boundary Conditions

A cyclical enthalpy boundary condition for the surface can be simulated with

$$\begin{aligned} H_s &= c_i(T_s - T_0), \\ T_s &= T_{avg} + \alpha \sin(\omega t), \end{aligned}$$

where α is the amplitude of temperature variation and $\omega = 2\pi/spy$ is the frequency. The surface-density boundary condition can be likewise described as (see Figure 1):

$$\rho_s^{n+1} = \rho_b^{n+1} d_p + \rho_s^n (1 - d_p).$$

The velocity of the surface can be described as

$$w_s = -\frac{\dot{b}}{\rho_s}, \quad \dot{b} = \rho_i \dot{a},$$

Where \dot{a} is the accumulation rate in $\text{m} \cdot \text{s}^{-1}$. The age of the firm on the surface will always be 0. Each of these of these can be created with FEniCS by

```
code = 'c*(Tavg + 9.9*sin(omega*t) - T0)'
Hs = Expression(code, c=cp, Tavg=Tavg,
                omega=freq, t=t0, T0=T0)
```

```
code = 'dp*rhon + (1 - dp)*rhoi'
rhoS = Expression(code, rhon=rhosi,
                  rhoi=rhosi, dp=1.0)
```

```
code = '- (rhoi * adot / spy) / rhos'
wS = Expression(code, rhoi=rhoi,
                adot=adot, spy=spy,
                rhos=rhos)
```

```
ageS = Constant(0.0)
```

```
def surface(x, on_boundary):
    return on_boundary and x[0] == zs
```

```
Hbc = DirichletBC(MV.sub(0), Hs, surface)
Dbc = DirichletBC(MV.sub(1), rhoS, surface)
wbc = DirichletBC(MV.sub(2), wS, surface)
ageBc = DirichletBC(V, ageS, surface)
```

Within the time-loop the variables in each Expression object can be updated as needed by utilizing the dot operator.

Now all that is left is to iterate through time and call the solve method at each step:

```
solve(f == 0, h, [Hbc, Dbc, wbc], J=J)
solve(f_a == 0, a, ageBc)
```

The solve function chooses *Newton's Method* by default to solve the non-linear enthalpy, density, and velocity residual by minimizing f . The boundary conditions are updated with these calls by specifying the list `[Hbc, Dbc, wbc]` and `ageBc` in solver parameters.

8 Model Parameters

Within the time-loop there are a number of parameters which need to be updated. Taking into account conservation of mass, the height l of each node must be recalculated:

$$l_{new} = l_{ini} \frac{\rho_{ini}}{\rho},$$

where ρ_{ini} and l_{ini} are the density and height vectors of the firn column when the system was initialized. With the height of the nodes calculated, the z-positions may be found by iterating through the heights and setting the z vector's corresponding cell equal to the current sum. These tasks may be completed with the following code performed by the `update_height` function of the `firn` class:

```
lnew = self.l*self.rho_in / self.rho
zSum = self.zb
zTemp = np.zeros(self.n)
for i in range(self.n)[1:]:
    zTemp[i] = zSum + lnew[i]
    zSum += lnew[i]
self.z = zTemp
```

The variable `index` is an array of positions corresponding to the correct ordering of the nodes, necessary after mesh refinement.

The height z_o at time index n of the original surface may be calculated as follows:

$$z_o^n = (z_s^0 - z_b) \frac{z_o^{n-1} - z_b}{z_s^{n-1} - z_b} + w_{z_o} \Delta t.$$

This maintains the relative location of the original surface to the current surface and moves downward proportional to w . This is accomplished in the class named `firn` with

```
interp = interp1d(self.z, self.w,
                  bounds_error=False,
                  fill_value=self.w[0])

zint = np.array([self.zo])
wzo = interp(zint)[0]
dt = self.dt
zs = self.z[-1]
zb = self.z[0]
zs_1 = self.zs_1
zo = self.zo
self.zo = (zs - zb) * (zo - zb) / (zs_1 - zb)
          + wzo * dt
```

The indexes to `self.z` refers to the surface, `[-1]`, or the base, `[0]`. For all operations it is convenient to store all the state data from the simulation in an object for ease of access. It was for this purpose the `firn` class was created and contains the signature

```
firn(data, z, l, index, dt)
```

with `data` a tuple containing the main variables, `z` the node z-positions as defined above, `l` the height vector of the elements, `index` the index of re-ordered mesh locations, and `dt` the time step of the program, Δt .

The variables for accumulation and surface temperature are the main driving forces in the simulation, and data from a specific site may be used in the model by interpolating the data in increments of Δt and inserting the values into the equations. This may be accomplished with the `set_local(n)` method of the `vector` class, which takes as input a NumPy array `n` with indexes corresponding to node positions within the mesh object. If the variable is used in the surface boundary condition, this may be updated within the FEniCS Expression object with the dot operator.

A function has been provided (`set_ini_conv`) which initializes the density to a previously derived density. The density may also be initialized to a set of real-world data if desired, and is demonstrated in the temperature equation model, `objModel.py`.

The `plot.py` file contains the class `firn` and the previously undescribed `plot` class. This class uses the

plotting package Matplotlib to display the data contained in the `firn` object. The method `plot_all_height()` plots the height history for a group of simulations and is useful for comparing the effects of model parameters.

Another version of `enthModel`, the main simulation class, has been created which uses collected data for density and surface temperature. When using this version, it is important to make Δt less than or equal to the time interval of recorded events so all data points are included.

9 Variable Definitions

Many variable are used in this simulation and many do not change. These are defined below:

Constants :

Var.	Value	Units	Description
g	9.81	m s^{-2}	gravitational acceleration
R	8.3144621	$\text{J mol}^{-1} \text{K}^{-1}$	gas constant
spy	31556926	s	seconds per year
ρ_i	917	kg m^{-3}	density of ice
ρ_w	1000	kg m^{-3}	density of water
ρ_m	550	kg m^{-3}	critical density value
k_i	2.1	$\text{W m}^{-1} \text{K}^{-1}$	thermal conductivity of ice
c_i	2009	$\text{J kg}^{-1} \text{K}^{-1}$	heat capacity of ice
L_f	3.34×10^5	J kg^{-1}	latent heat of fusion
H_s	$c_i(T_w - T_0)$	J kg^{-1}	Enthalpy of ice at T_w
T_w	273.15	K	triple point of water
T_0	0.0	K	reference temperature
k_g	1.3×10^{-7}	$\text{m}^2 \text{s}^{-1}$	grain growth coefficient
E_c	60×10^3	J mol^{-1}	act. energy for water in ice
E_g	42.4×10^3	J mol^{-1}	act. energy for grain growth

Variables used by the model can be specified to suit simulation requirements:

Model Specific :

Var.	Units	Description
ρ_s	kg m^{-3}	initial density at surface
\dot{b}	$\text{kg m}^{-2} \text{s}^{-1}$	surface accumulation
A	mm a^{-1}	surface accumulation
V_a	m s^{-1}	mean annual wind speed
T_{avg}	K	average annual temperature
T_s	K	firn surface temperature
z_s	m	surface start z-location
z_b	m	firn base z-location
z_{s1}	m	previous time-step's surface
dz	m	initial z-spacing
l	m	vector of node heights
Δt	s	time-step
t_0	s	begin time
t_f	s	end-time

10 Verification of Program

A converging run of the program was done quickly by making Δt equal `spy`: this has the effect of producing a

steady-state solution. After the density-profile converged the data was saved to a text file in the `data` folder. The script was run again with the average surface air temperature T_{avg} made so that the surface temperature peaks at 8°C if $t < 10$ years, and 0°C if $t \geq 10$ years. This has the effect of halting any melting and refreezing after this time period. For this run the method `set_ini_conv` was called to initialize the previous runs data and Δt was set to $0.0025 * spy$; the results are shown in Figures 2 and 3.

11 Interpretation

The surface-density equation has two values for new accumulation: ρ_s and ρ_w depending on the 2-meter average surface air temperature. This is quite simplified; a better approach that models real-life circumstances can be found.

Testing with real-world temperature and accumulation data-sets is required to validate the model. The simulation's surface-height- and density-profile outputs while using these data may then be compared against cataloged surface-height and density-profile data to verify its accuracy.

Above the ice lens in Figure 2 you will see numerical distortion: this is caused by the sudden rise in density where the lens begins. This distortion is a source of inaccuracies and needs also to be corrected.

12 Work in Progress

At its current state of development the model does not take into account water transport through the firn column, describable with the Darcy flow equations:

$$q = \frac{-k}{\mu} \nabla P, \quad v = \frac{q}{\phi},$$

where k is permeability, $\mu = 1.787 \times 10^{-3} \text{ Pa}\cdot\text{s}$ is the viscosity of water at 0°C , ∇P is the pressure gradient vector, and $\phi = 1 - \rho/\rho_i$ is porosity.

Waldner *et al.* [2002] introduces this issue and provides references to numerous models which simulate this phenomenon. Coleou *et al.* [1998] supplies an equation for the irreducible water content of snow

$$S_0 = \frac{0.0057}{1 - \phi} + 0.0017,$$

which may be used with the expression for permeability from Bozhinskiy & Krass [1989] :

$$k = k_0 \exp(m\phi) \left(\frac{S - S_0}{\phi - S_0} \right)^2,$$

where S is the relative water content and k & m are empirical constants.

13 Concluding Remarks

This model is a good start towards accurately modeling the densification of firn: it uses the work of many established models and has the potential to expand; The simulation is able to assimilate data easily, is mathematically easy to interpret, and runs efficiently. This subject is a worthy candidate for further study.

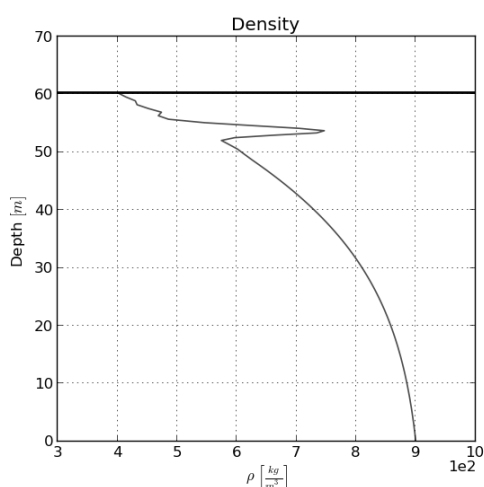


Figure 2: Density profile after 40 years with an ice lens approximately 7 meters below the surface

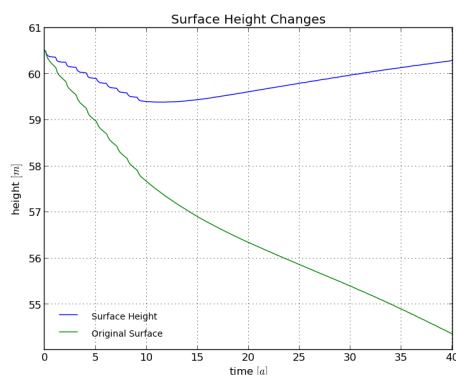


Figure 3: 40-year height history of the column (blue) and original surface (green) resulting in the previous figure. This shows a rapid decrease in height as the lens is formed in the first ten years of simulation. The fluctuations in height show an increase in height with winter temperatures.

References

- Aschwanden, A., Bueler, E., Khroulev, C., and Blatter, H. 2012. An enthalpy formulation for glaciers and ice sheets. *J. Glaciol.* **58**(209), 441-457.
- Paterson, W.S.B. 1994. *The physics of glaciers*, 3rd edn. Elsevier, Oxford.
- Arthern, R.J., Vaughan, D.G., Rankin, A.M., Mulvaney, R., and Thomas, E.R. 2010. In situ measurements of Antarctic snow compaction compared with predictions of models. *J. Geophys. Res.*, **115**, FO3011, doi:10.1029/2009JF001306.
- Reeh, N. 2008. A nonsteady-state firn-densification model for the percolation zone of a glacier. *J. Geophys. Res.*, **113**, F03023, doi:10.1029/2007JF000746.
- Zwally, H. and J. Li. 2002. Seasonal and interannual variations of firn densification and ice-sheet surface elevation at the Greenland summit. *J. Glaciol.* **48**(161), 199-207.
- Ligtenberg, S.R.M., Helsen, M.M., and van den Broeke, M.R. 2011. An improved semi-empirical model for the densification of Antarctic firn. *The Cryosphere*. **5**, 809-819. doi:10.5194/tc-5-809-2011.
- Coleou, C. and Lesaffre, B. 1998. Irreducible water saturation in snow: experimental results in a cold laboratory. *Ann. Glaciol.*, **26**, 64-68.
- Herron, M. and Langway, C. 1980. Firn densification: an empirical model. *J. Glaciol.* **25**(93), 373-385.
- Waldner, P.A., Schneebeli, M., Schultze - Zimmermann, U., and Flüher, H. 2002. Effect of snow structure on water flow and solute transport. *Hydrol. Process.*, DOI: 10.1002/hyp.1401
- Bozhinskiy, A.N. and Krass, M.S. 1989. A mathematical model of snowmelt and water percolation processes in snow and firn. *Snow Cover and Glacier Variations*. IAHS publ. no. 183.
- Logg, A., Mardal, K., and Wells, G.N. 2011. *Automated Solution of Differential Equations by the Finite Element Method*, The FEniCS Project.
- Codina, R. 1997. Comparison of some finite element methods for solving the diffusion-convection-reaction equation, *Comput. Methods Appl. Mech. Engrg.*, **156**(1998), 185-210.